Santacatalina Bonet, JV.; Fissore, D.; Carcel Carrión, JA.; Mulet Pons, A.; García Pérez, JV. (2015). Model-based investigation into atmospheric freeze drying assisted by power ultrasound. Journal of Food Engineering. 151:7-15. doi:10.1016/j.jfoodeng.2014.11.013.

MODEL-BASED INVESTIGATION INTO ATMOSPHERIC FREEZE DRYING ASSISTED BY POWER ULTRASOUND

J.V. Santacatalina[1], D. Fissore[2], J.A. Cárcel[1], A. Mulet[1] and J.V. García-Pérez[1]*

[1]Grupo ASPA, Departamento de Tecnología de Alimentos, Universitat Politècnica de València, Camí de Vera s/n, E46022, València, Spain.

[2]Dipartimento di Scienza Applicata e Tecnologia, Politecnico di Torino, corso Duca degli Abruzzi 24, 10129 Torino, Italy.

*Corresponding author. Tel.: +34 963879376; fax: +34 963879839. E-mail address: jogarpe4@tal.upv.es (J.V. García-Pérez).

Abstract

Atmospheric freeze drying consists of a convective drying process using air at a temperature below the freezing point of the processed product, and with a very low relative humidity content. This paper focuses on the use of a simple one-dimensional model considering moving boundary vapor diffusion to describe the ultrasonic assisted atmospheric freeze-drying of foodstuffs. The case study is the drying of apple cubes (8.8 mm) at different air velocities (1, 2, 4 and 6 m/s), temperatures (-5, -10 and -15ºC), without and with (25, 50 and 75 W) power ultrasound application. By fitting the proposed diffusion model to the experimental drying kinetics, the effective diffusivity of water vapor in the dried product was estimated. The model was successfully validated by drying apple samples of different size and geometry (cubes and cylinders). Finally, a 2^3 factorial design of experiments revealed that the most relevant operating parameter affecting the drying time was the applied ultrasound power level.

Keywords:

Atmospheric freeze-drying, ultrasound, modeling, optimization.

1. Introduction

Atmospheric freeze drying (AFD) consists of a convective drying process where the temperature of the air has to be kept below the freezing point of the processed material, and the relative humidity has to be, in general, very low. Since the air is not saturated with water vapor, a vapor partial pressure gradient is created between the product and the air, forcing the ice to sublimate and the water vapor to diffuse to the air (Meryman, 1959; Bantle & Eikevik, 2011). AFD is generally carried out at temperatures of between -10ºC and the initial freezing point of the product, as this appears to be a good compromise between costs and final product quality (Wolff & Gibert, 1990a, 1990b; Claussen et al., 2007a, 2007b). The advantages of AFD are its lower cost compared to vacuum freeze drying and the possibility of its being carried out as a continuous process, thus also allowing energy recovery (Bantle et al., 2011)

In cold regions, the AFD process has a long history of use as a means of food preservation (Rhamann & Mujumdar, 2008a), although Meryman (1959) was the first to report the potential of AFD. Stawczyk et al. (2007) investigated the freeze-drying kinetics and the product quality of apple cubes in a fully automated heat pump-assisted drying system. Their results showed that the rehydration kinetics and the hygroscopic properties of the product were similar to those obtained by vacuum freeze drying. These findings agreed with the work of Claussen et al. (2007c), which was carried out using heat pump fluidized bed and tunnel dryers. However, despite the promises of low energy consumption and a better quality product, certain problems still exist in the atmospheric freeze-drying process, limiting its practical implementation. Furthermore, due to the low vapor diffusivity at atmospheric pressure, AFD is controlled by the internal resistance to heat and mass transfer, making it a long drying process (Rhamann & Mujumdar, 2008b).

Since the main drawback of the AFD process is the low sublimation rate, improving mass transfer would be beneficial. In the last few years, new power transducers with

66 extensive surface radiators have been developed for applications in gas media
67 (Gallego-Juárez et al., 2001), such as de-foaming and air drying. Thus, high-intensity
68 airborne ultrasound application brings about mechanical effects when the sound wave
69 is directed into the product (Bhaskaracharya et al., 2009), which intensify the drying of
70 foodstuffs (Gallego-Juarez et al., 2007; Gallego-Juarez, 2010; Riera et al., 2011).
71 Therefore, high-intensity airborne ultrasound was suggested as a potential technology
72 for improving mass transfer in AFD by Cárcel et al. (2011). Ozuna et al. (2014) and
73 García-Perez et al. (2012) have also shown the feasibility of employing power
74 ultrasound to accelerate the drying kinetics of fruits, vegetables and fish at low
75 temperatures. The latter have achieved a maximum drying time reduction of 77% by
76 applying power ultrasound during the drying of apple at -10ºC.

77 Mathematical modeling represents an important tool in the analysis of the drying
78 process and the operation of the dryer (Mulet et al., 2010). Several empirical, semi-
79 empirical, and analytical equations have been reported for predicting the drying curves
80 for different products and operating conditions. However, there are few first principle
81 models which have been reported to thoroughly describe the AFD process and even
82 less effort has been made to assess its adequacy. One of these models is based on
83 the Lewis equation and its accuracy depends greatly on the accurate evaluation of the
84 thermal properties in the structure of the dried product (Claussen et al., 2007b).
85 Rahman et al. (2009) also suggested a method based on the thermal properties of the
86 product and used the analogy between Nusselt and Sherwood numbers to predict the
87 drying rate in AFD. A similar approach was taken by Li et al. (2007), where a CFD
88 model for an AFD process of apple was developed. When also working on the AFD of
89 apple cubes, Stawczyk et al. (2007) observed that no first drying stage or constant
90 drying rate occurred, and the complete dehydration process was controlled by internal
91 water diffusivity. A similar conclusion was also drawn by Di Matteo et al. (2003). An
92 analytical solution for AFD is presented by Wolff & Gibert (1990a, 1990b) where the

93 ‘‘Uniformly Retreating Ice Front’’ (URIF) approach is coupled to the laws of heat and
94 mass transfer. In the URIF model, the product is divided into two layers; a frozen (or
95 wet) inner core and an outer dry layer. It is assumed that the drying occurs as a
96 consequence of the frozen core gradually shrinking down to zero. Heat is transported
97 from the surface of the product, causing sublimation at the ice front. The resulting water
98 vapor is transported back to the surface and to the gas medium.

99 In this context, the main goals of this work were to evaluate the feasibility of a simple
100 one-dimensional model to describe the ultrasonic assisted AFD process of apple
101 cubes, as well as to validate such a model in different operating conditions. Finally, a
102 suitable design of experiments coupled with the analysis of the effects was used to
103 point out the key parameter for the atmospheric freeze drying process, which would
104 positively contribute to further optimization stages.

105

106 **2. Materials and methods**

107 *2.1. Raw material*

108 Apples (*Malus domestica* cv. Granny Smith) were purchased in a local market
109 (Valencia, Spain). Fruits were selected to obtain a homogeneous batch in terms of
110 ripeness, size and color, and held at 4ºC until processing. Cubic samples (8.8 mm and
111 17.5 mm side) were obtained from the flesh using a household tool. Cylindrical
112 samples (height 40 mm and diameter 15 mm) were also prepared using a 15 mm hole
113 puncher. All the samples were wrapped in plastic film and frozen at -18±1ºC until
114 processing (at least 24 h). The initial moisture content was measured by placing the
115 samples in a vacuum oven at 70ºC and 200 mmHg until constant weight was reached,
116 following the standard method 934.06 (AOAC, 1997).

117

118 *2.2. Drying experiments*

Drying experiments were carried out in a convective drier with air recirculation (Figure 1), already described in the literature (García-Pérez et al., 2012). The drier provides an automatic temperature and air velocity control. A cylindrical radiator (internal diameter 100 mm, height 310 mm, thickness 10 mm) driven by a power ultrasonic transducer (frequency 22 kHz, power capacity 90 W) was used as the drying chamber. The transducer generates an ultrasonic field inside the cylinder, which interacts with the samples and the surrounding air during drying. Air goes through the cylindrical radiator where samples were randomly placed in a holder for assuring a uniform treatment of them for both air flow and ultrasound application. A set of experiments was carried out to determine the drying kinetics of apple cubes (8.8 mm) at different air velocities (1, 2, 4 and 6 m/s), temperatures (-5, -10 and -15ºC), without and with (25, 50 and 75 W) power ultrasound (US) application. Another set of experiments was carried out with larger apple cubes (17.5 mm). In this case, the drying conditions used were -10ºC, 2 m/s and without US application.

In every experiment, the samples were weighed at preset times and the relative air humidity was kept at under 15±5%. For each run, the initial mass load density was 9.5 kg/m^3. The drying experiments were extended until the samples lost 80% of the initial weight. Every condition was tested in triplicate, at least.

Finally, a third drying test was carried out using apple cylinders, whose surface was kept isolated with a plastic film, with the exception of one of the flat surfaces. So, the water vapor outlet took place in only one direction. The samples were dried at -15°C, 2 m/s and without US application. In order to determine the moisture profile for different percentages of weight loss (10, 20, 30 and 40%), the cylinder was split into 5 equal sections and the individual moisture content of each section was determined following the standard method 934.06 (AOAC, 1997).

2.3. Mathematical modeling

As previously mentioned, the Uniformly Retreating Ice Front (URIF) model has been used to model the atmospheric freeze-drying of foodstuffs. Assuming cubic samples behave as spherical bodies (Figure 2A) during AFD, the mass balance for the water vapor in the dried product is given, in steady-state conditions, by the following equation:

$$\frac{d}{dr}\left(r^2 J_w\left(r\right)\right)=0 \tag{1}$$

where the water flux is given by the well- known Fourier equation:

$$J_w\left(r\right)=-\frac{D_e M_w}{RT}\frac{dp_w\left(r\right)}{dr} \tag{2}$$

The integration of eq. (1), using eq. (2) and the following boundary conditions:

$$\begin{array}{ll} r=L_0-L_{dried} & p_w=p_{w,i} \\ r=L_0 & p_w=p_w^* \end{array} \tag{3}$$

gives:

$$p_w\left(r\right)=\frac{1}{r}\left(\frac{p_{w,i}-p_w^*}{L_{dried}}\right)L_0\left(L_0-L_{dried}\right)+\left[p_w^*-\frac{1}{L_0}\left(\frac{p_{w,i}-p_w^*}{L_{dried}}\right)L_0\left(L_0-L_{dried}\right)\right] \tag{4}$$

From eq. (4), it is possible to calculate the sublimation flux (using eq. (2)), thus obtaining:

$$J_w\left(r\right)=\frac{D_e M_w}{RT}\frac{1}{r^2}\left(\frac{p_{w,i}-p_w^*}{L_{dried}}\right)L_0\left(L_0-L_{dried}\right) \tag{5}$$

and, finally, the sublimation flow rate:

$$G=4\pi r^2 J_w\left(r\right)=\frac{D_e M_w}{RT}4\pi\frac{L_0\left(L_0-L_{dried}\right)}{L_{dried}}\left(p_{w,i}-p_w^*\right) \tag{6}$$

The mass flow rate from the surface of the sample to the drying chamber is also given by the following equation: G

$$G = S\alpha \frac{M_w}{RT}\left(p_w^* - p_{w,c}\right) \quad (7)$$

Using eqs. (6) and (7) it is possible to calculate the sublimation flow rate in the following way:

$$G = \frac{M_w}{RT} \frac{1}{\frac{1}{S\alpha} + \frac{L_{dried}}{4\pi D_e L_0 (L_0 - L_{dried})}} \left(p_{w,i} - p_{w,c}\right) \quad (8)$$

where $p_{w,i}$, the partial pressure of water at the interface of sublimation is a well- known function of the temperature.

Following exactly the same approach, it is possible to calculate the heat flow rate in the dried layer by means of the following equation:

$$Q = \frac{1}{\frac{1}{S\beta} + \frac{L_{dried}}{4\pi\lambda_{dried} L_0 (L_0 - L_{dried})}} \left(T_{air} - T_i\right) \quad (9)$$

All the energy transferred into the product is used for ice sublimation and, thus:

$$Q = G\Delta H_s \quad (10)$$

Equation (10) can be used to calculate the interface temperature, given the values of the operating conditions, of the heat and mass transfer coefficients, of product parameters D_e and λ_{dried}, and of the dried layer thickness. Then, it is possible to calculate the sublimation flow rate (using eq. (8)) and the evolution of the dried volume:

$$\frac{dV_{dried}}{dt} = \frac{G}{\rho_{dried}\left(W_0 - W_f\right)} \quad (11)$$

and, finally, of the residual amount of ice in the sample:

$$-\frac{dW}{dt} = \rho_{dried}\left(W_0 - W_f\right)\frac{dV_{dried}}{dt} \quad (12)$$

In the case of planar geometry, as shown in Figure 2, graph B, exactly the same approach can be followed. Thus, the mass balance for the water vapor in the dried product is given, in steady-state conditions, by the following equation:

$$\frac{d}{dx}\left(J_w\left(x\right)\right)=0 \tag{13}$$

with the following boundary conditions:

$$\begin{array}{ll} x=L_0-L_{dried} & p_w=p_{w,i} \\ x=L_0 & p_w=p_w^* \end{array} \tag{14}$$

and the water flux is given by the Fourier equation:

$$J_w\left(x\right)=-\frac{D_e M_w}{RT}\frac{dp_w\left(x\right)}{dx} \tag{15}$$

After some calculations, it is possible to obtain the following equation to calculate the sublimation flow rate:

$$G=\frac{M_w}{RT}\frac{1}{\frac{1}{\alpha}+\frac{L_{dried}}{D_e}}\left(p_{w,i}-p_{w,c}\right) \tag{16}$$

and the heat flow rate in the dried layer is given by the following equation:

$$Q=\frac{1}{\frac{1}{\beta}+\frac{L_{dried}}{\lambda_{dried}}}\left(T_{air}-T_i\right) \tag{17}$$

In this case, it is also possible to assume that all the energy transferred into the product is used for ice sublimation, i.e. eq. (10) and, thus calculating the interface temperature from the values of the operating conditions, heat and mass transfer coefficients, product parameters D_e and λ_{dried}, and dried layer thickness. Then, the sublimation flow rate (using eq. (16)) and the evolution of the dried layer thickness can be estimated:

$$\frac{dL_{dried}}{dt}=\frac{G}{\rho_{dried}S(W_0-W_f)} \tag{18}$$

202 and, finally, of the residual amount of ice in the sample:

203 $$-\frac{dW}{dt} = S\rho_{dried}(W_0 - W_f)\frac{dL_{dried}}{dt} \quad (19)$$

204 As regards the estimation of heat and mass transfer coefficients, α and β, several
205 equations can be found in the literature. Among others, Krokida et al. (2002) reported
206 various empirical equations with which to calculate the coefficient β, given as a function
207 of the air Reynolds number:

208 $$j_h = aRe^n \quad (20)$$

209 while the Lewis equation is used to calculate the coefficient α:

210 $$\alpha = \frac{\beta}{\rho_{air} c_{p,air}} \quad (21)$$

211 In any case, the atmospheric freeze-drying process appears to be controlled by the
212 internal resistance to water vapor transfer in most cases, as is also reported by Bantle
213 et al. (2011) for the AFD process of peas, and as also pointed out in this study for
214 apple drying; thus, the correlations used to calculate α and β do not significantly affect
215 the accuracy of the results. The constant parameters used in the AFD modeling
216 of apple cubes and cylinders are included in Table 1.

217

218 *2.4. Design of experiments*

219 In order to assess the effect of the various operating parameters, namely air
220 temperature, air velocity and ultrasound application, on drying time, a standard Design
221 of Experiments (DoE) technique was used. This aims to investigate the reciprocal
222 interactions among the variables, and to find those which play the major role in the
223 drying kinetics (Montgomery, 2005). In particular, a 2^3 factorial design of experiments
224 was used to evaluate how air temperature (factor A), air velocity (factor B), and
225 acoustic power (factor C) affect the drying time. High (+) and low (-) values of these

parameters (factor A: -10 and -5°C, factor B: 2 and 6 m/s and factor C: 0 and 50 W) were considered, as is graphically illustrated in Figure 3, where these eight combinations are represented by lowercase letters of the alphabet. Lowercase letters indicate that the parameter is at the high level, for the sake of clarity: a identifies the combination of A at the high level (-5°C) and B and C at the low level (2 m/s and 0 W), ab identifies the combination of A and B at the high level (-5°C and 6 m/s) and C at the low level (0 W), abc identifies the combination of A, B and C at the high level (-5°C, 6 m/s, 50 W) while (1) identifies the combination of A, B and C at the low level (-10°C, 2 m/s and 0 W). Then, the single effects of various parameters can be calculated. For example, the effects of A are:

- $\left[a-(1)\right]/n$ when the values of B and C are both low;
- $\left[ab-b\right]/n$ when the value of B is high and the value of C low;
- $\left[ac-c\right]/n$ when the value of C is high and the value of B low and
- $\left[abc-bc\right]/n$ when the values of B and C are both high,

where n is the number of repetitions of the test. By averaging the previously calculated single effects, the total effect of A, also known as the contrast parameter, on the drying time is obtained:

$$A=\frac{1}{4n}\left[a-(1)+ab-b+ac-c+abc-bc\right]=\frac{Contrast_A}{4n} \quad (22)$$

Similarly, the effects of parameters B and C can be calculated, as well as the interactions between these factors. The effect can be positive or negative: if the value is positive, when the parameter increases (from the minimum to the maximum) the observed variable (the drying time) also increases, and vice versa when the value is negative. Finally, the percentage contribution of each factor to the drying time can be determined. The analysis of variance “ANOVA” was carried out using the Fisher test to

verify the significance of the differences between the arithmetic means of the various groups.

3. Results and discussion

3.1. Assessment of model adequacy and water diffusivity estimation

The drying kinetics of apple cubes (8.8 mm side) processed at different velocities (1, 2, 4 and 6 m/s), temperatures (-15, -10 and -5°C), and without and with (25, 50 and 75 W) power ultrasound application were modeled using the equations described in the previous sections. For modeling purposes, a spherical geometry has been assumed for the food samples, and the sphere diameter has been determined in such a way that the product volume is the same as that of the cubic samples. The value of water effective diffusivity in the dried product (D_e) has been determined by looking for the best fit between the calculated and measured values of the residual moisture in the product vs time.

For every combination of the operating conditions under investigation, the model was observed to fit the experimental data very well, as can be observed in Figure 4. Claussen et al. (2007b) also used the URIF model to simulate the AFD of apple, turnip, cabbage and cod pieces, exhibiting a good agreement with the experimental data (not shown), whereas Li et al. (2007) found some differences between the experimental values and those calculated by means of the URIF model at the beginning of the AFD of apple cubes. Using the same approach, Reyes et al. (2010) reported a 10% deviation of the model for the AFD of berries.

As regards the values of the water vapor effective diffusivity in the dried product, this study permitted the effect of the different operating parameters (temperature, air velocity and applied acoustic power) on D_e and, thus, on drying kinetics to be demonstrated. Air temperature was observed to have a significant ($p<0.05$) effect on

276 the identified D_e (Table 2): the higher the temperature used, the higher the D_e value.
277 This influence of temperature was also observed in the US-assisted experiments. As
278 for the effect of air velocity, as expected, it has no effect on the estimated value of D_e
279 (Table 3) when US is not applied. Otherwise, for drying experiments conducted with
280 US application, a slightly lower D_e was identified for the experiments carried out at the
281 highest air velocities tested (4 and 6 m/s); however, no significant ($p<0.05$) differences
282 were observed. This fact could be due to some disruption of the ultrasonic field caused
283 by the turbulences produced by high air flow velocities, reducing the acoustic intensity
284 that reaches the sample, as reported by García-Pérez et al. (2006). Low air flow rates
285 should not affect the ultrasonic field, thus a major fraction of ultrasonic energy would
286 be available to increase water vapor diffusivity into the sample. In every case, the
287 obtained D_e values were much higher (6 orders of magnitude) than those computed by
288 Santacatalina et al. (2014) and Li et al. (2008) for AFD apple kinetics when using a
289 strict diffusion model and identifying the liquid water diffusivity.

290 As regards the US application, the increase in the level of applied acoustic power led
291 to a rise in the effective diffusivity (Table 4). It should also be remarked that the lowest
292 power tested (25 W) allowed a huge increase (370%) in the D_e value to be obtained
293 (Table 4). Therefore, it is illustrated that US application is very effective at accelerating
294 the AFD experiments, even when using a low acoustic power. Several effects of
295 ultrasonic waves to improve mass diffusion in solid matrix have been reported
296 (Gallego-Juárez, 1998). In this sense, US produce series of cyclical and rapid (>20
297 kHz) compressions and expansions, a mechanism known as sponge effect; this
298 alternating stress creates microscopic channels that help to make the movement of
299 water vapor from the ice front towards the product surface easier. In addition,
300 ultrasound may also contribute to the water sublimation since, to a certain extent, the
301 attenuation of the acoustic wave may provide the energy needed for the water to
302 change state (Gallego-Juárez, 2010).

303 The obtained results are interesting because, just by using a low acoustic power, the
304 amount of energy consumed by an AFD experiment could be reduced (due to the
305 shorter drying time) and the degradation of the structure of the sample could be
306 minimal. In this sense, Puig et al. (2012) have analyzed the microstructure of eggplant
307 and how it is affected by the application of US during its drying at 40ºC and have
308 reported that the lowest acoustic power tested (45 W) provoked less degradation than
309 when US was applied at its maximum power capacity (90 W).

310

311 *3.2. Model validation*

312 A first attempt to validate the model consisted of using the diffusivities identified for
313 each one of the drying conditions tested to predict the drying times and compare them
314 to the experimental times. Since the air velocity did not have a significant effect on the
315 value of the diffusivity for the experiments conducted without US application, an
316 average D_e value was used to simulate the drying kinetics at the four air velocities
317 tested so it could be further compared to the experimental results (Figure 5). It may be
318 observed that the experimental and calculated times were very similar for every
319 condition tested.

320 Moreover, a more rigorous model validation was addressed by carrying out additional
321 experiments to those used to identify the diffusivity values. Thus, the diffusivity value
322 obtained in the experiments performed on apple cubes of 8.8 mm side (at -10°C, 2 m/s
323 and without US application) to model a drying experiment carried out under the same
324 drying conditions, but on different-sized samples: cubes of 17.6 mm side. As can be
325 observed in Figure 6, experimental data were quite similar to those simulated.

326 Model validation was also performed with a third set of experiments under completely
327 different experimental conditions. In this case, atmospheric freeze drying experiments
328 were carried out on apple cylinders, 40 mm in height and 15 mm in diameter, which

were water-proof isolated to behave as infinite slabs of 40 mm, as already mentioned in section 2.2. The D_e obtained from the experiments performed on apple cubes (8.8 mm side) under the same experimental conditions (2 m/s, -15°C, without US application) was used to model apple cylinder experiments. The evolution of the moisture profile was calculated using the model, taking into account the position of the sublimation front at every time in order to estimate the moisture of each one of the five sections of apple cylinders. Figure 7 depicts the reasonably good match between the experimental moisture of the sections and the computed value. Therefore, the moisture profile in the samples confirmed the assumptions considered in the model, as well as the results obtained. In Figure 7, it may be seen how the sublimation front moves from the surface of the sample in contact with the air, leaving a dry layer through which water vapor diffuses onto the surface. Meanwhile, the frozen area maintained the initial moisture content ($W/W_0 = 1$) and shrank as drying progressed. These retreating ice fronts have also been observed by Crespi et al. (2008) when analyzing paper samples that had previously been soaked in distilled water and freeze-dried for different times by immersing the partially dried sample in a dye that colored the ice (wet zone). However, as far as we are concerned, the experimental validation of the URIF model showing the location of the ice front has not been reported for foodstuffs.

3.3. Analysis of the effects

The process variables considered in this study were temperature, air velocity and ultrasound application. In order to quantify the effect of these operating variables on the AFD times, a set of experiments was performed. Two levels (high and low) of each variable were selected to make a two-level factorial design (2^3), with three replicates from each run. The contribution percentages of each factor to the drying time and their interactions are shown in Figure 8. It can be observed that the variable with the most relevant effect on the drying time was US application, followed by temperature and the

356 interaction between them. The effect of air velocity appears to be negligible under
357 these drying conditions, as has previously been mentioned. Therefore, for the drying
358 conditions studied in this design, the key parameter is US application. Consequently,
359 this parameter should be conveniently modified to optimize the drying process.

360

361 **4. Conclusions**

362 In this study, a simple one-dimensional model has been successfully applied to assess
363 the effect of the US application on the AFD kinetics of apple. US severely shortened
364 the drying time under every condition tested. On the other hand, the model has been
365 validated under different drying conditions (different size and geometry of the sample)
366 obtaining a good fit to the experimental data and showing the retreat of the ice front
367 during AFD. From a 2^3 factorial design of experiments, it has been proven that US
368 application is the parameter with the greatest influence on the AFD time and,
369 consequently, is the key factor for the further optimization of the process.

370

371 **Acknowledgements**

372 The authors acknowledge the financial support of the Spanish Ministerio de Economia
373 y Competitividad (MINECO) and of the European Regional Development Fund (ERDF)
374 through the project DPI2012-37466-CO3-03, the FPI fellowship (BES-2010-033460)
375 and the EEBB-I-14-08572 fellowship granted to J.V. Santacatalina for a short stay at
376 Politecnico di Torino.

377

378 **List of symbols**

379 S surface of the product, m^2

380 a parameter used to calculate the heat transfer coefficient

381	$c_{p,air}$	air specific heat, J/kg K
382	D_e	effective diffusivity of water vapor in the dried product, m^2/s
383	G	sublimation flow rate, kg/s
384	ΔH_s	heat of sublimation, J/kg
385	J_w	sublimation flux, kg/s m^2
386	j_h	*j-factor* for the heat transfer
387	L_0	initial characteristic dimension of the product, m
388	L_{dried}	characteristic dimension of the dried product, m
389	M_w	water molecular weight, kg/kmol
390	n	parameter used to calculate the heat transfer coefficient
391	p_w	water vapor partial pressure, Pa
392	$p_{w,c}$	water vapor partial pressure in the drying chamber, Pa
393	$p_{w,i}$	water vapor partial pressure at the sublimation interface, Pa
394	p_w^*	water vapor partial pressure at the external surface of the product, Pa
395	Q	heat flow rate, W
396	R	ideal gas constant, J/kmol K
397	Re	Reynolds number
398	r	radial coordinate
399	T	temperature, K
400	T_{air}	air temperature, K
401	T_i	temperature of the sublimation interface, K
402	t	time, s

403 V_{dried} volume of the dried product, m^3

404 W water content in the product, $kg_{water}/kg_{dry\ matter}$

405 W_0 water content in the product at the beginning of the drying process,
406 $kg_{water}/kg_{dry\ matter}$

407 W_f water content in the product at the end of the drying process,
408 $kg_{water}/kg_{dry\ matter}$

409 x axial coordinate, m

410

411 Greek letters

412 α mass transfer coefficient, m/s

413 β heat transfer coefficient, $W/m^2\ K$

414 λ_{dried} thermal conductivity of the dried product, W/m K

415 ρ_{air} density of the air, kg/m^3

416 ρ_{dried} density of the dried product, kg/m^3

417

418 **References**

419 Association of Official Analytical Chemists (AOAC) (1997). Official methods of analysis.
420 Association of Official Analytical Chemists, Arlington, Virginia, USA.

421 Bantle, M., & Eikevik, T.M. (2011). Parametric study of high intensity ultrasound in the
422 atmospheric freeze drying of peas. *Drying Technology, 29*, 1230-1239.

423 Bantle, M., Kolsaker, K., & Eikevik, T.M. (2011). Modification of the Weibull distribution
424 for modeling atmospheric freeze-drying of food. *Drying Technology, 29*, 1161-
425 1169.

426 Bhaskaracharya, R.K., Kentish, S., & Ashokkumar, M. (2009). Selected applications of
427 ultrasonics in food processing. *Food Engineering Reviews, 1,* 31-49.

428 Cárcel, J.A., García-Pérez, J.V., Peña, R., Mulet, A., Riera, E., Acosta, V., & Gallego-
429 Juárez, J.A. (2011). Procedimiento y dispositivo para mejorar la transferencia
430 de materia en procesos a baja temperatura mediante el uso de ultrasonidos de
431 elevada intensidad. International patent, Spanish ref. P201131512.
432 Internacional PCT ref. 120120283, September 20.

433 Claussen, I.C., Ustad, T.S., Strømmen, I., & Walde, P.M. (2007a). Atmospheric freeze
434 drying - A review. *Drying Technology, 25,* 957-967.

435 Claussen, I.C., Andresen, T., Eikevik, T.M., & Strømmen, I. (2007b). Atmospheric
436 freeze drying - Modeling and simulation of a tunnel dryer. *Drying Technology,*
437 *25,* 1959-1965.

438 Claussen, I.C., Strømmen, I., Torstveit Hemmingsen, A.K., & Rustad, T. (2007c).
439 Relationship of product structure, sorption characteristics, and freezing point of
440 atmospheric freeze-dried foods. *Drying Technology, 25,* 853-865.

441 Crespi, E., Capolongo, A., Fissore, D., & Barresi, A. (2008). Experimental investigation
442 of the recovery of soaked paper using evaporative freeze drying. *Drying*
443 *Technology, 26,* 349-356.

444 Di Matteo, P., Donsì, G., & Ferrari, G. (2003). The role of heat and mass transfer
445 phenomena in atmospheric freeze-drying of foods in a fluidized bed. *Journal of*
446 *Food Engineering, 59,* 267-275.

447 Gallego-Juárez, J.A. (1998). Some applications of air-borne power ultrasound to food
448 processing. In: *Ultrasound in Food Processing*, Povey, M.J.W., & Mason,
449 T.J. Eds., Thomson Science, London, UK, 127-143.

Gallego-Juárez, J.A., Yang, T., Vázquez-Martínez, F., Gálvez-Moraleda, J.C., & Rodríguez-Corral, G. (2001). Dehydration method and device. US Patent, ref. 6233844 B1, May 22.

Gallego-Juárez, J.A., Riera, E., de la Fuente-Blanco, S., Rodríguez-Corral, G., Acosta-Aparicio, V.M., & Blanco, A. (2007). Application of high-power ultrasound for dehydration of vegetables: processes and devices. *Drying Technology, 25*, 1893-1901.

Gallego-Juárez, J.A. (2010). High-power ultrasonic processing: Recent developments and prospective advances. *Physics Procedia, 3*, 35-47.

García-Pérez, J.V., Cárcel, J.A., de La Fuente-blanco, S., & Riera-Franco de Sarabia, E. (2006). Ultrasonic drying of foodstuff in a fluidized bed: Parametric study. *Ultrasonics, 44,* e539-e543.

García-Pérez, J.V., Cárcel, J.A., Riera, E., Rosselló, C., & Mulet, A. (2012). Intensification of low temperature drying by using ultrasound. *Drying Technology, 30*, 1199-1208.

Krokida, M.K., Maroulis, Z.B., & Marinos-Kouris, D. (2002). Heat and mass transfer coefficients in drying: Compilation of literature data. *Drying Technology, 20,* 1-18.

Li, S., Stawczyk, J., & Zbicinski, I. (2007). CFD model of apple atmospheric freeze drying at low temperature. *Drying Technology, 25*, 1331-1339.

Li, S., Zbicinski, I., Wang, H., Stawczyk, J., & Zhang, Z. (2008). Diffusion model for apple cubes atmospheric freeze-drying with the effect of shrinkage. *International Journal of Food Engineering, 6*, 1-7.

Meryman, H.T. (1959). Sublimation: Freeze-drying without vacuum. *Science, 130,* 628-629.

475 Montgomery, D.C. (2005). *Design and analysis of experiments*, 7th ed., John Wiley and
476 Sons, New York, USA.

477 Mulet, A., Cárcel, J.A., Sanjuán, N., & García-Pérez, J.V. (2010). Food dehydration
478 under forced convection conditions. In: Recent Progress in Chemical
479 Engineering, J. Delgado ed., Studium Press LLC, Houston, TX, USA.

480 Ozuna, C., Cárcel, J.A., Walde, P.M. & García-Pérez, J.V. (2014). Low-temperature
481 drying of salted cod (Gadus morhua) assisted by high power ultrasound:
482 Kinetics and physical properties. *Innovative Food Science and Emerging*
483 *Technologies, 23*, 146-155.

484 Puig, A., Pérez-Munuera, I., Cárcel, J.A., Hernando, I., & García-Pérez, J.V. (2012).
485 Moisture loss kinetics and microstructural changes in eggplant
486 (Solanummelongena L.) during conventional and ultrasonically assisted
487 convective drying. *Food and Bioprocess Processing, 90*, 624-632.

488 Rahman, S. (2009). A novel approach on atmospheric freeze drying. Lambert
489 Academic Publishing, Köln, Germany.

490 Reyes, A., Bubnovich, V., Bustos, R., Vásquez, M., Vega, R., & Scheuermann, E.
491 (2010). Comparative study of different process conditions of freeze drying of
492 ‘‘Murtilla’’ berry. *DryingTechnology, 28,* 1416-1425.

493 Rhamann, S.M.A., & Mujumdar, A.S. (2008a). Vacuum and atmospheric freeze drying.
494 In: *Guide to Industrial Drying - Principles, Equipments and New Developments,*
495 Mujumdar, A.S., Ed., Colour Publications Ltd., Hyderabad, India.

496 Rhamann, S.M.A., & Mujumdar, A.S. (2008b). A novel atmospheric freeze-drying
497 system using a vibro-fluidized bed with adsorbent. *DryingTechnology, 26,* 393-
498 403.

499 Riera, E., García-Pérez, J.V., Acosta, V.M., Cárcel, J.A., & Gallego-Juárez, J.A. (2011).
500 A computational study of ultrasound-assisted drying of food materials. In:

501 *Multiphysics Simulation of Emerging Food Processing Technologies,* Knoerzer,
502 K., Juliano, P., Roupas, P., & Versteeg,C., Eds., IFT Press, Chicago, USA, 265-
503 302.

504 Santacatalina, J.V., Rodríguez, O., Simal, S., Cárcel, J.A., Mulet, A., & García-Pérez,
505 J.V. (2014). Ultrasonically enhanced low-temperature drying of apple: Influence
506 on drying kinetics and antioxidant potential. *Journal of Food Engineering, 138,*
507 35-44.

508 Stawczyk, J., Li, S., Witrowa-Rajchert, D., & Fabisiak, A. (2007). Kinetics of
509 atmospheric freeze-drying of apple. *Transport in porous media, 66,* 159-172.

510 Wolff, E., & Gibert, H. (1990a). Atmospheric freeze drying. Part 1: Design, experimental
511 investigation and energy-saving advantages. *Drying Technology, 8,* 385-404.

512 Wolff, E., & Gibert, H. (1990b). Atmospheric freeze drying. Part 2: Modelling drying
513 kinetics using adsorption isotherms. *Drying Technology, 8,* 405-428.

514

Figure captions

Figure 1. Scheme of the ultrasonically assisted convective drier: 1, fan; 2, Pt-100; 3, temperature and relative humidity sensor; 4, anemometer; 5, ultrasonic transducer; 6, vibrating cylinder; 7, sample load device; 8, retreating pipe; 9, slide actuator; 10, weighing module; 11, heat exchanger; 12, heating elements; 13, desiccant tray chamber; 14, details of the sample load on the trays.

Figure 2. Sketch of a partially freeze-dried product with spherical (A) and planar (B) geometry.

Figure 3. Graphical representation of the 2^3 factorial design used to investigate the effect of air temperature (A), of air velocity (B), and of ultrasonic application (C) on the drying time.

Figure 4. Comparison between the evolution of the residual amount of water in the product measured experimentally (symbols) and calculated using the mathematical model of the process (lines) during atmospheric freeze-drying of apple samples (air temperature: -10°C, air velocity: 2 m/s) without ultrasound (A) and with ultrasound application (50 W, B).

Figure 5. Comparison between the experimentally measured (empty bars) and the calculated (grey bars) values of the time required to reduce the amount of water in the sample by 50% (A) and by 90% (B) during atmospheric freeze-drying of apple samples as a function of air velocity (air temperature: -10°C), without ultrasound application.

Figure 6. Comparison between the evolution of the residual amount of water in the product measured experimentally (symbols) and calculated using the mathematical

543 model of the process (lines) during atmospheric freeze-drying of apple samples (17.6
544 mm side, air temperature: -10°C, air velocity: 2 m/s) without ultrasound application.
545
546 **Figure 7.** Comparison between the experimentally measured (empty bars) and the
547 calculated (grey bars) values of the residual amount of water in the product at different
548 axial positions (given as distance from the isolated flat surface; x_1 = 0.036 m, x_2 =
549 0.028 m, x_3 = 0.02 m, x_4 = 0.012 m, x_5 = 0.004 m) during atmospheric freeze-drying of
550 apple samples (air temperature: -10°C, air velocity: 2 m/s, without ultrasound
551 application), for different total weight loss (graph A: 10%, graph B: 20%, graph C: 30%,
552 graph D: 40%).
553
554 **Figure 8.** Contribution percentages of the process variables to the duration of the
555 atmospheric freeze-drying of apple samples (A: temperature; B: air velocity; C: acoustic
556 power).

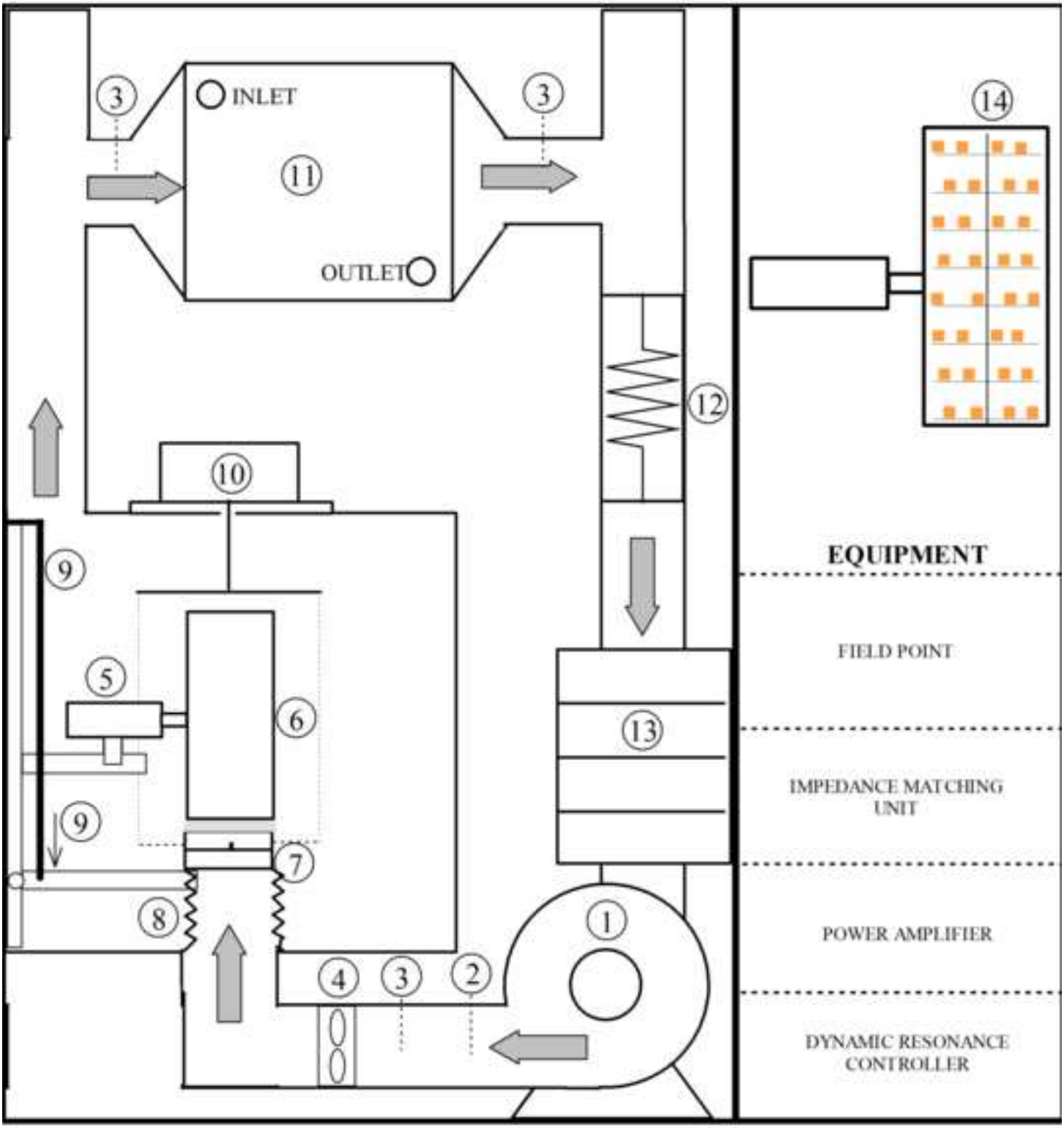
INLET
OUTLET
EQUIPMENT
FIELD POINT
IMPEDANCE MATCHING UNIT
POWER AMPLIFIER
DYNAMIC RESONANCE CONTROLLER

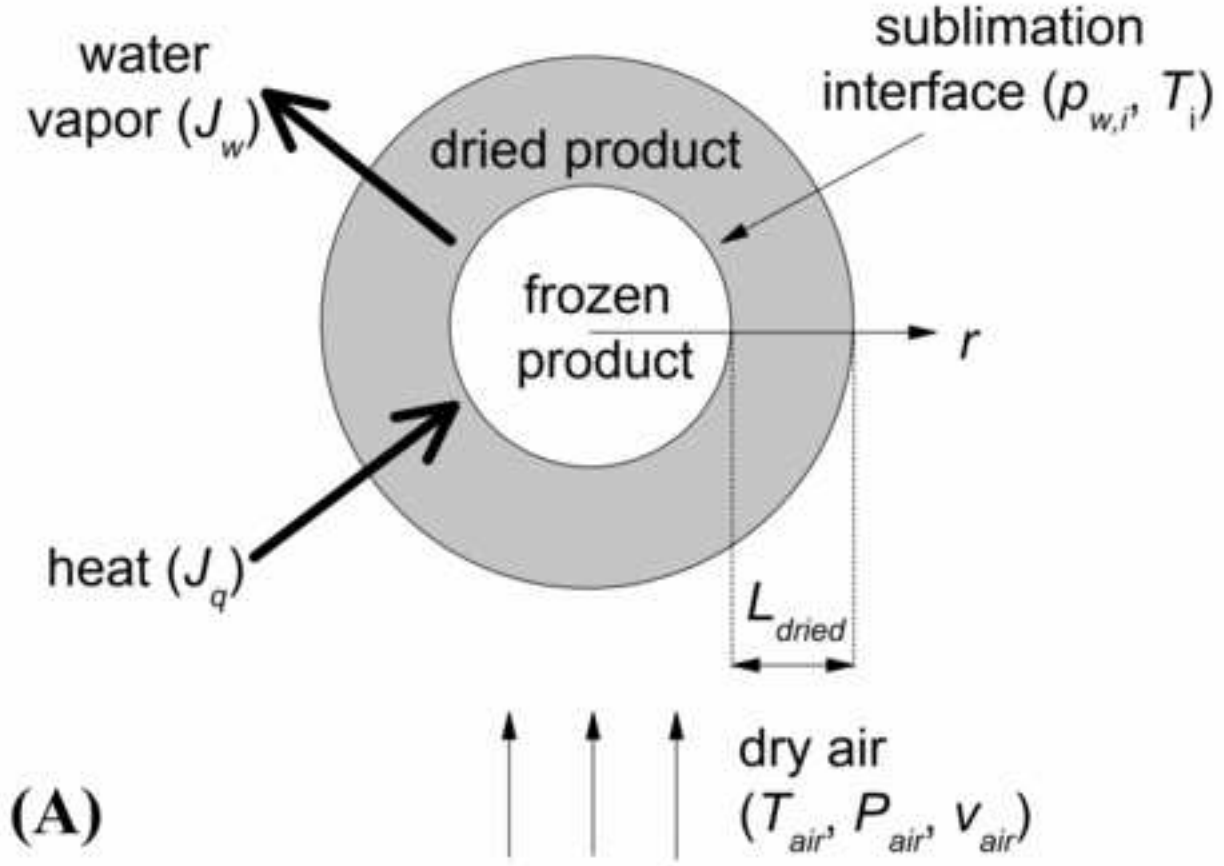
water
vapor (J_w)
sublimation
interface ($p_{w,i}$, T_i)
dried product
frozen
product
r
heat (J_q)
L_{dried}
dry air
(T_{air}, P_{air}, v_{air})
(A)

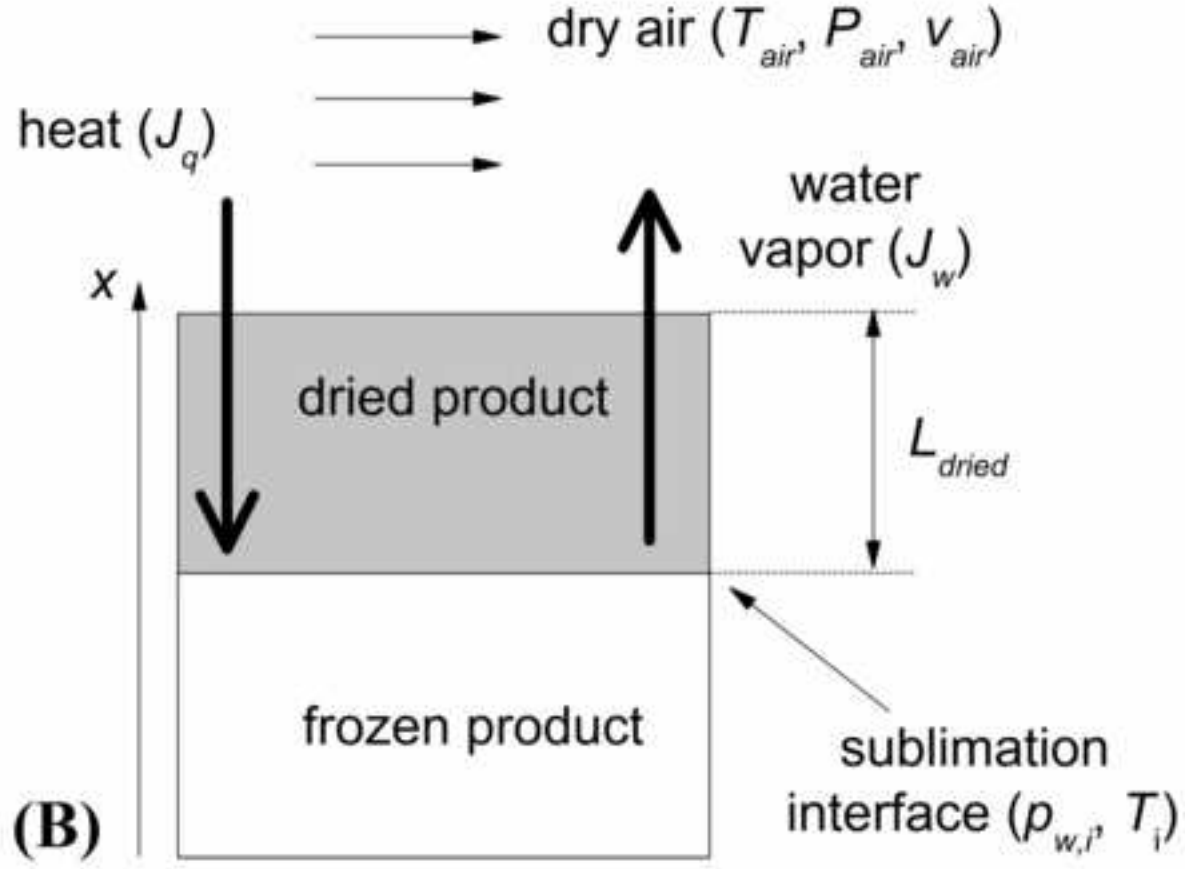
dry air (T_{air}, P_{air}, v_{air})
heat (J_q)
water
vapor (J_w)
x
dried product
L_{dried}
frozen product
sublimation
interface ($p_{w,i}$, T_i)
(B)

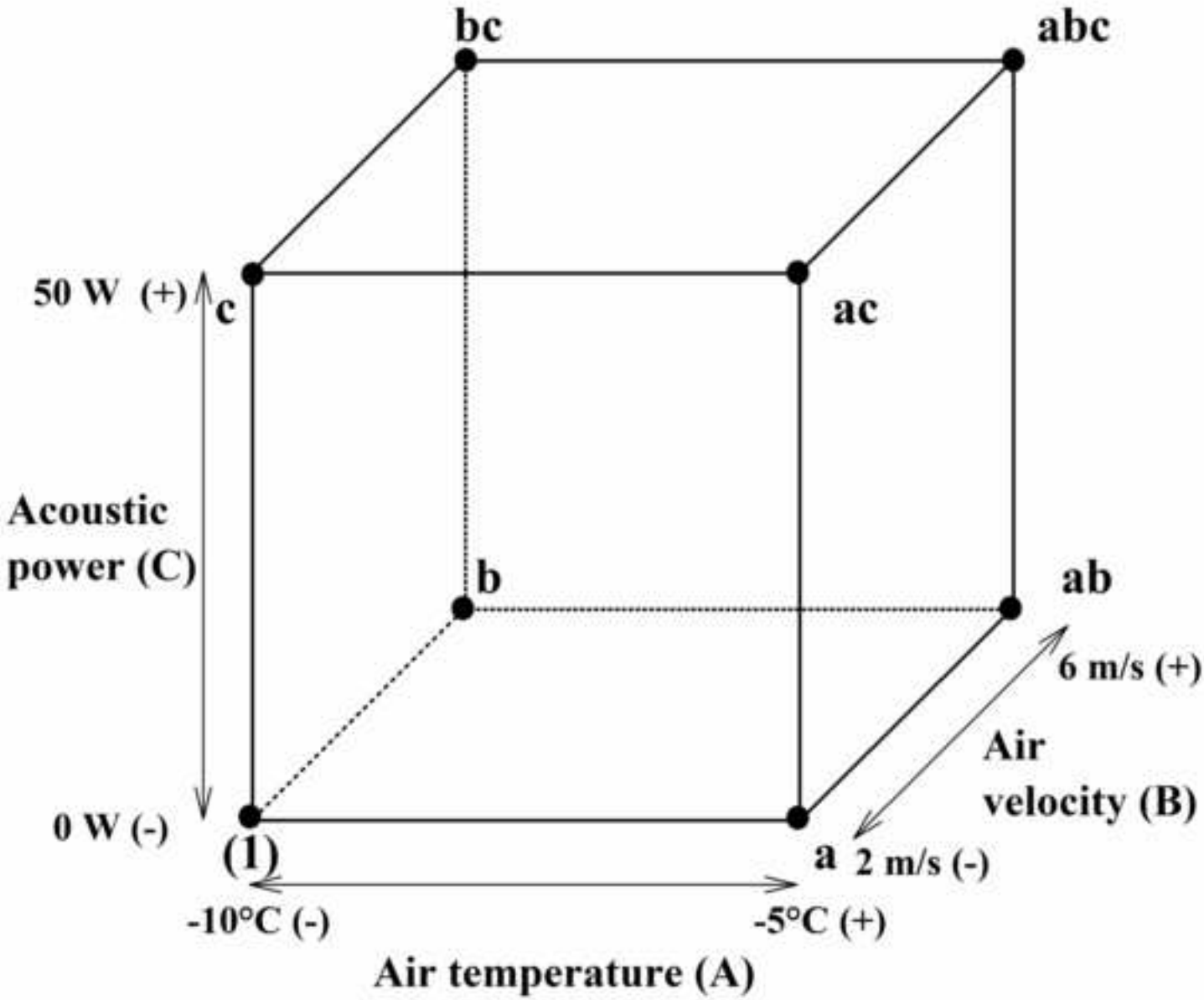
bc
abc
50 W (+)
c
ac
Acoustic
power (C)
b
ab
6 m/s (+)
Air
velocity (B)
0 W (-)
(1)
a
2 m/s (-)
-10°C (-)
-5°C (+)
Air temperature (A)

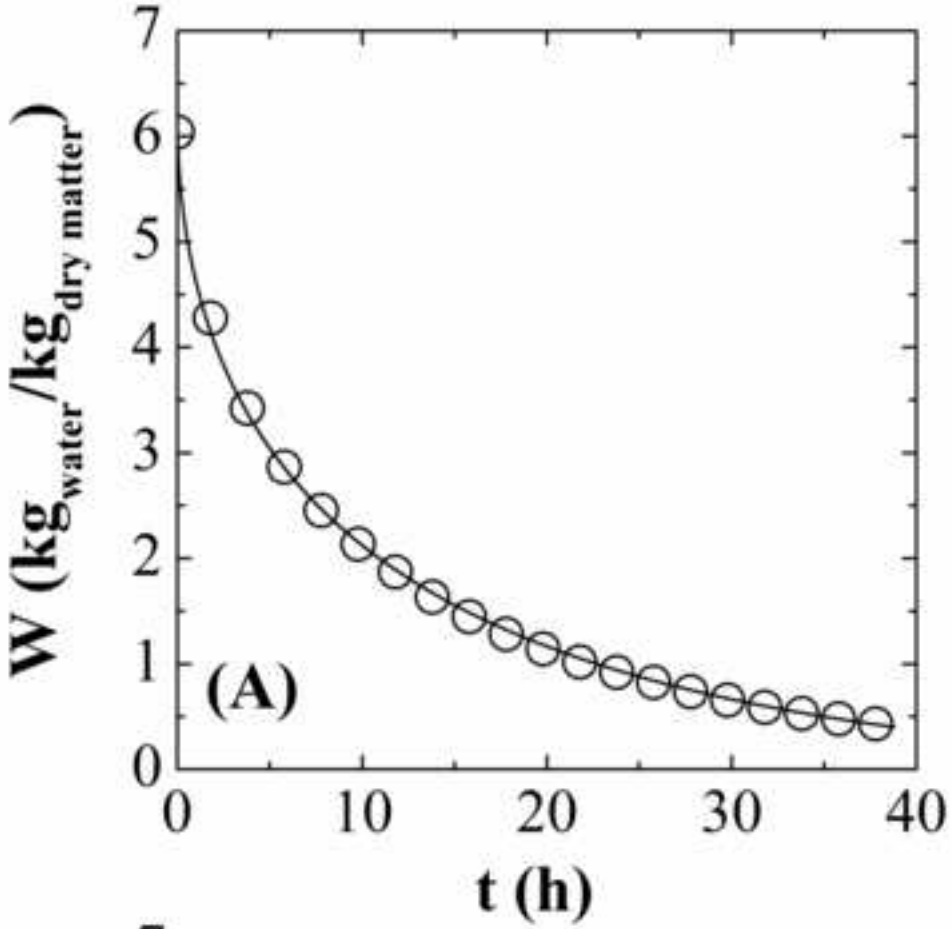
W (kg$_{water}$/kg$_{dry\ matter}$)
(A)
t (h)
0
1
2
3
4
5
6
7
0
10
20
30
40

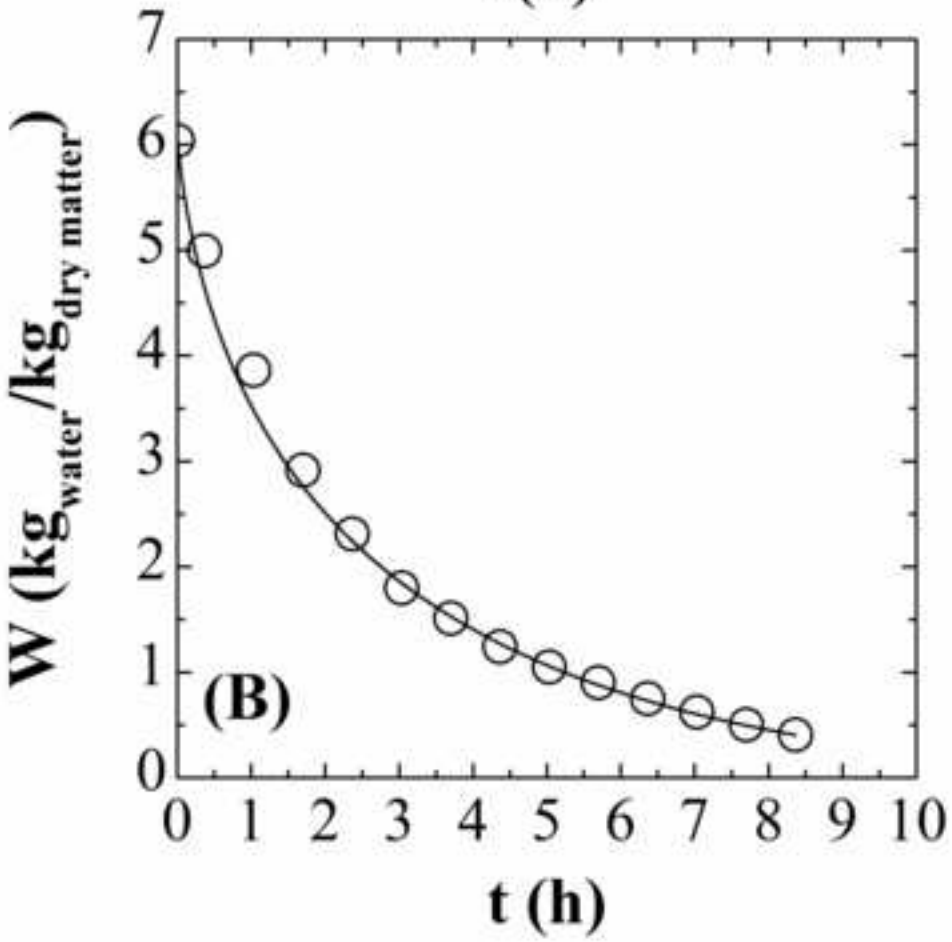
W (kg$_{water}$/kg$_{dry\ matter}$)
(B)
t (h)
0
1
2
3
4
5
6
7
0
1
2
3
4
5
6
7
8
9
10

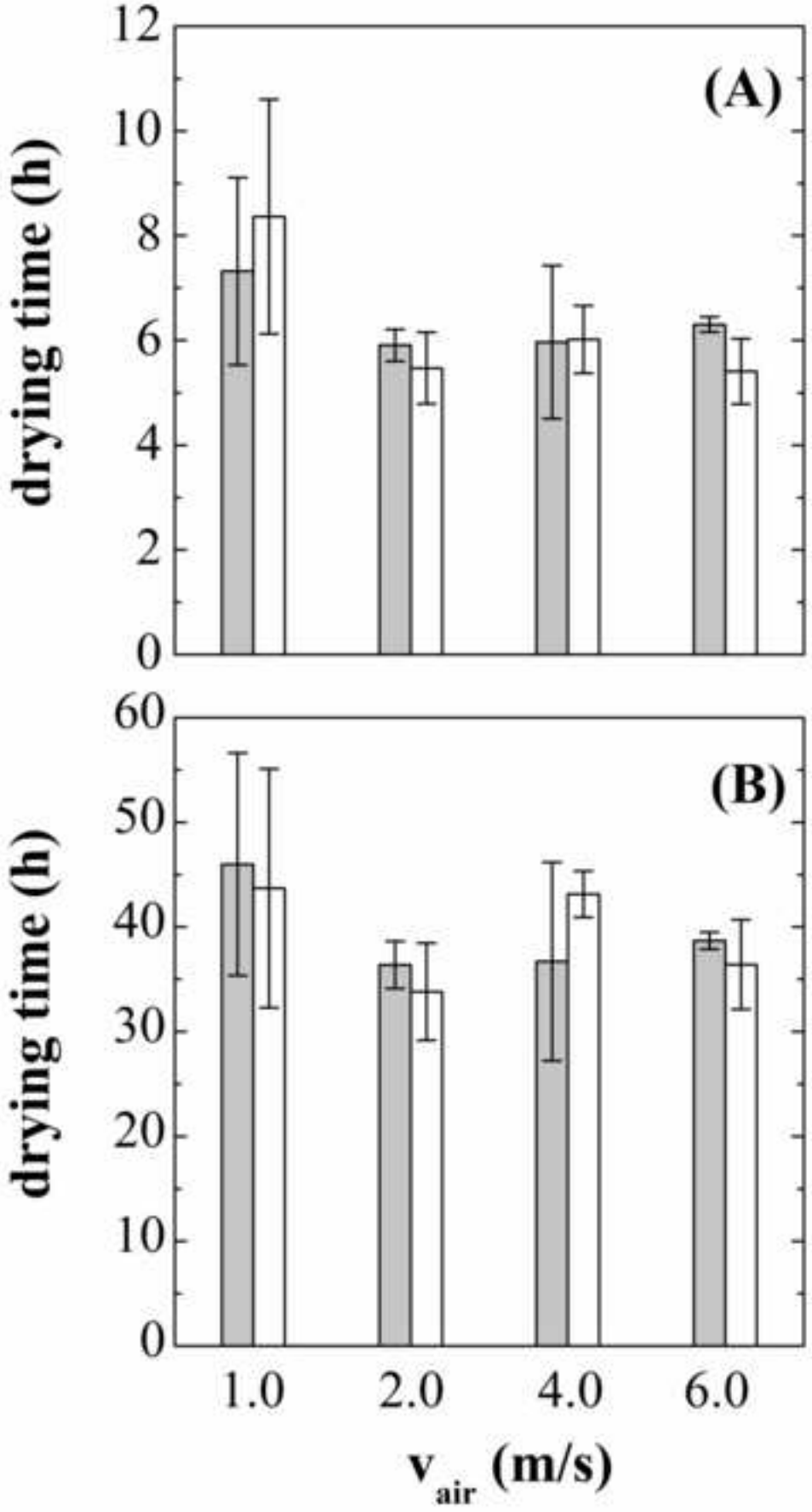
(A)
(B)
drying time (h)
drying time (h)
0
2
4
6
8
10
12
0
10
20
30
40
50
60
1.0
2.0
4.0
6.0
v air (m/s)

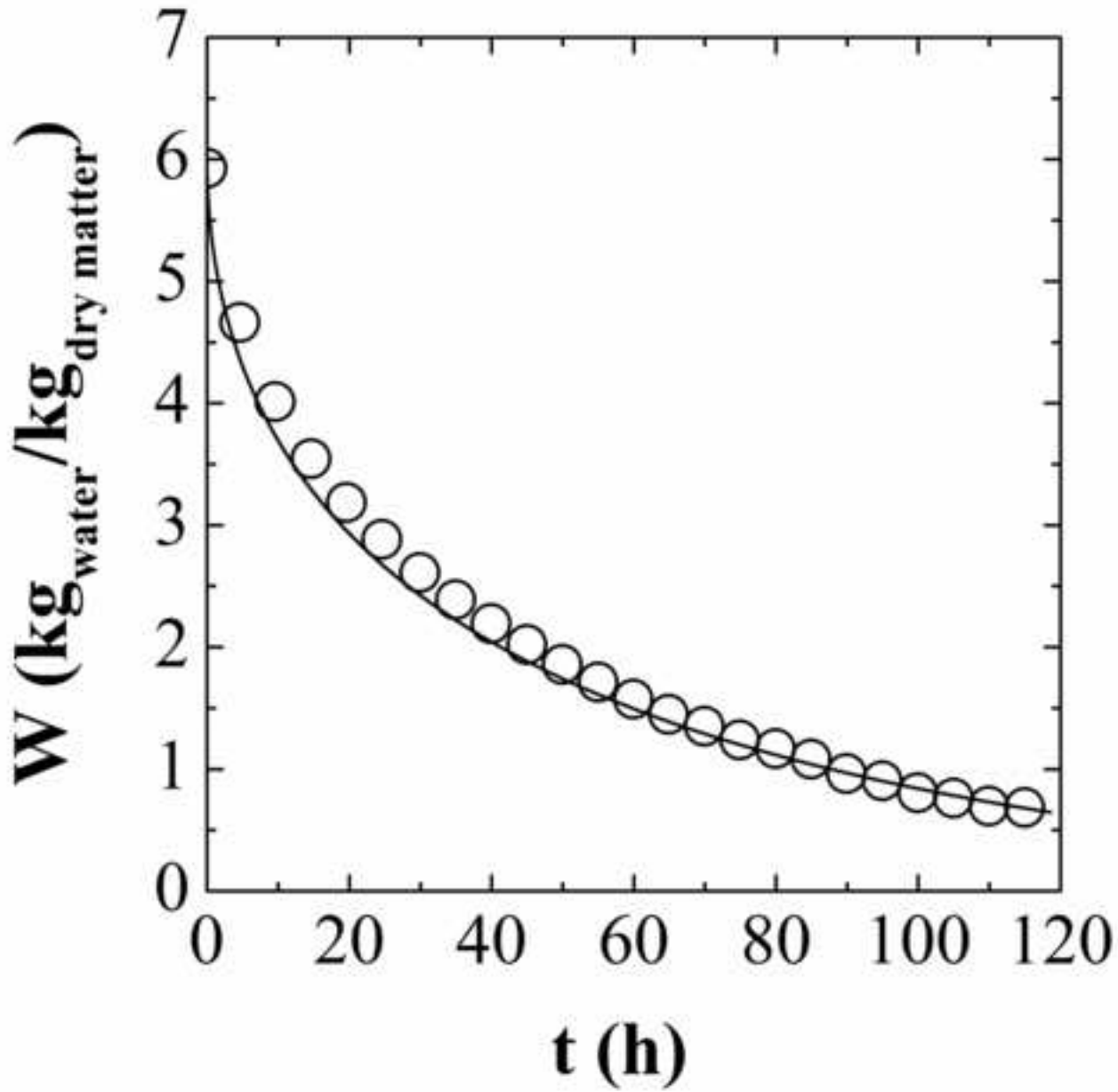
W (kg_water /kg_dry matter)
0
1
2
3
4
5
6
7
0
20
40
60
80
100
120
t (h)

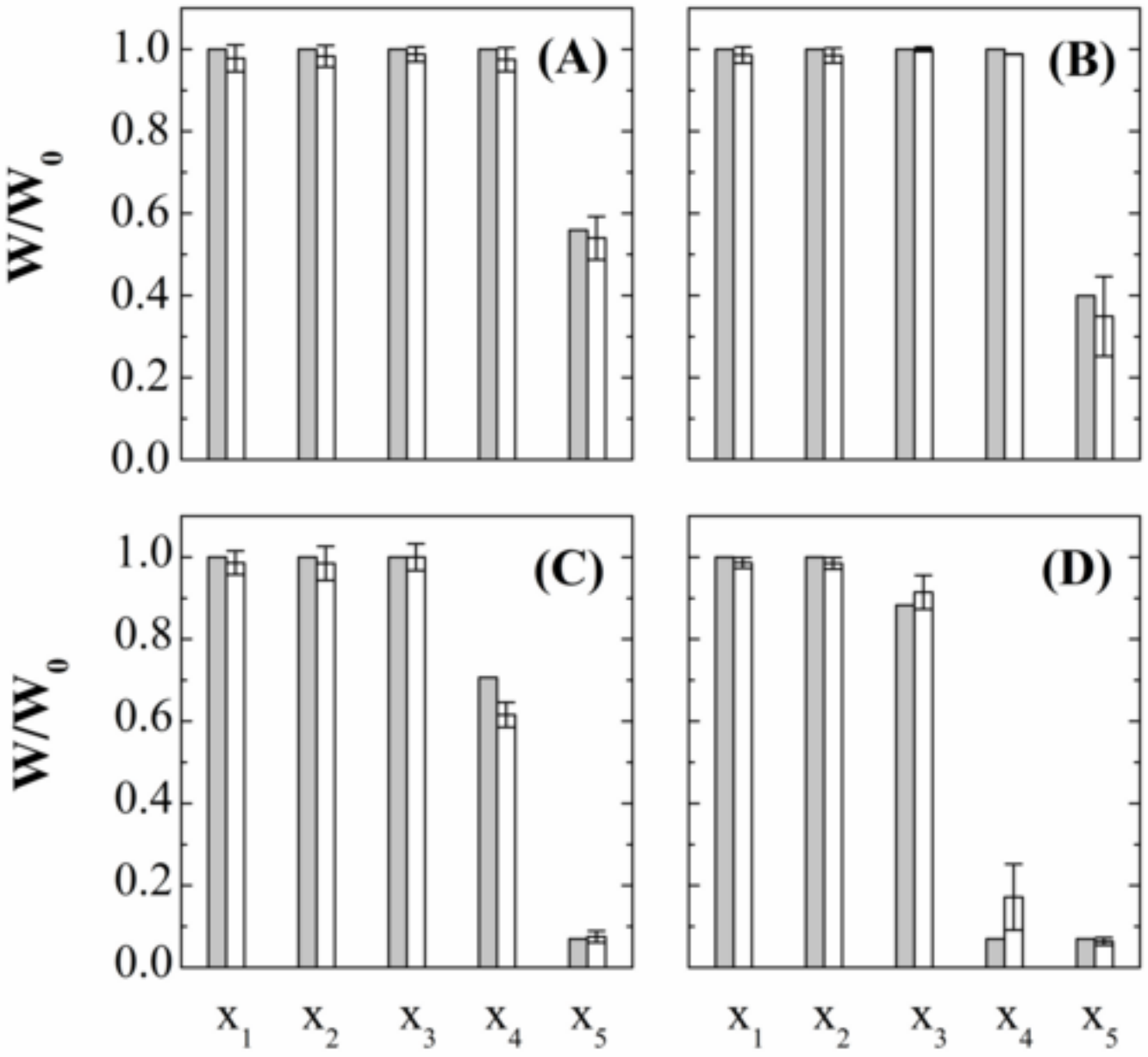
(A)
(B)
(C)
(D)
W/W0
1.0
0.8
0.6
0.4
0.2
0.0
x1
x2
x3
x4
x5

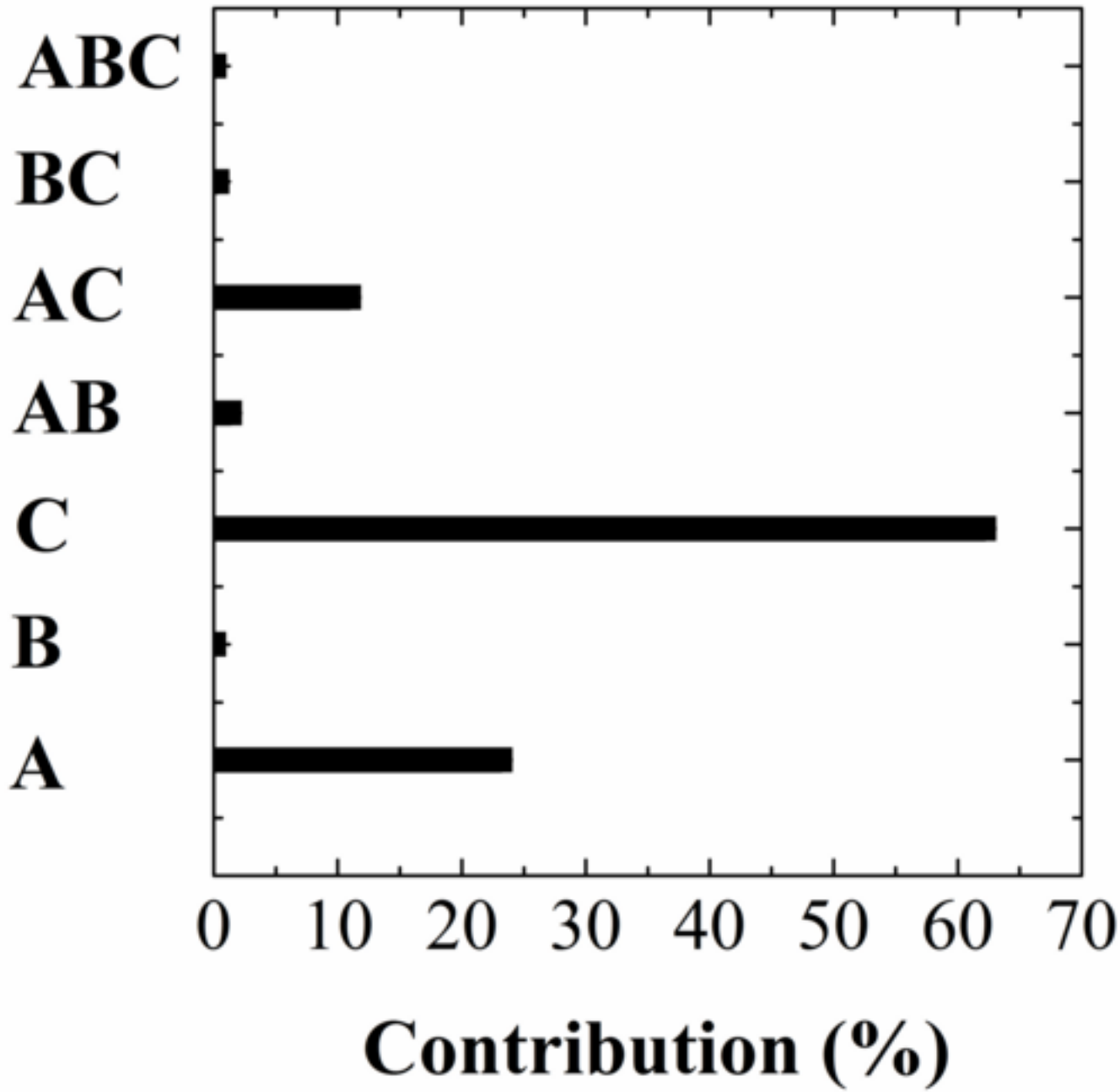
ABC
BC
AC
AB
C
B
A
0
10
20
30
40
50
60
70
Contribution (%)

Table 1

Table 1. Constant parameters used for the modeling of the atmospheric freeze drying kinetics of apple.

Parameter	Value
L_0, initial characteristic dimension (m) Spherical geometry	0.0044
Planar geometry	0.04
W_0, water content in the product at the beginning of the drying process ($kg_{water}/kg_{dry\ matter}$)	5.928
W_f, water content in the product at the end of the drying process ($kg_{water}/kg_{dry\ matter}$)	0.382
ρ_{dried} , **density of the dried product (kg/m^3)**	124.5
$\lambda_{dried,}$ thermal conductivity of the dried product (W/m K)	0.1
R, ideal gas constant (J/kmol K)	8.314
M_w, water molecular weight (kg/kmol)	18
$c_{p,air}$, air specific heat (J/kg K)	1005
a, parameter used to calculate the heat transfer coefficient	0.59
n, parameter used to calculate the heat transfer coefficient	-0.38

Table 2

Table 2. Effective diffusivities (D_e) identified from the modeling of apple drying kinetics at 2 m/s with (50 W) and without (0 W) power ultrasound application. Mean values ± standard deviation.

	D_e (10^{-5} m^2/s)	
	0 W	**50 W**
-5°C	1.61±0.12[a]	6.95±1.22[c]
-10°C	1.50±0.23[a]	6.70±1.03[c]
-15°C	1.08±0.09[b]	3.60±0.97[d]

Superscript letters (a, b) and (c, d) show homogeneous groups established from LSD (Least Significance Difference) intervals ($p<0.05$).

Table 3

Table 3. Effective diffusivities (D_e) identified from the modeling of apple drying kinetics at -10ºC with (50 W) and without (0 W) power ultrasound application. Mean values ± standard deviation.

	D_e (10^{-5} m^2/s)	
	0 W	**50 W**
1 m/s	1.38±0.10[a]	6.48±1.05[b]
2 m/s	1.50±0.23[a]	6.70±1.03[b]
4 m/s	1.34±0.62[a]	6.37±0.33[b]
6 m/s	1.50±0.16[a]	6.04±0.34[b]

Superscript letters (a, b) show homogeneous groups established from LSD (Least Significance Difference) intervals ($p<0.05$).

Table 4

Table 4. Effective diffusivities (D_e) identified from the modeling of apple drying kinetics at 2 m/s, -10ºC and different acoustic powers. Mean values ± standard deviation.

	D_e (10^{-5} m^2/s)
0 W	1.50±0.23[a]
25 W	5.54±0.33[b]
50 W	6.70±1.03[b]
75 W	12.24±1.05[c]

Superscript letters (a, b, c) show homogeneous groups established from LSD (Least Significance Difference) intervals ($p<0.05$).